Non-coherent CPM Detection under Gaussian Channel affected with Doppler Shift

Anouar Jerbi, Frédéric Guilloud, Karine Amis, Tarik Benaddi

Non-coherent CPM Detection under Gaussian Channel affected with Doppler Shift

Anouar Jerbi* †, Frédéric Guilloud*, *senior member IEEE*, Karine Amis*, *member IEEE*,
Tarik Benaddi‡
* IMT Atlantique, Lab-STICC, UMR CNRS 6285, 29238 Brest, France,
† TéSA, 31000 Toulouse, France,
‡ Thales Alenia Space, 31000 Toulouse, France
e-mails: {anouar.jerbi, frederic.guilloud, karine.amis}@imt-atlantique.fr, tarik.benaddi@thalesaleniaspace.com

***Abstract*—We consider the transmission of a continuous phase modulated (CPM) signal through a Gaussian channel affected by Doppler shifts. We propose a receiver robust to the Doppler shifts derived from a non-coherent detection criterion. We compare its performance to another non-coherent receiver based on a linear approximation of the CPM signal (Laurent decomposition) to which we add a Doppler compensation. Simulation results show that the first algorithm is robust to low-moderate Doppler shifts, while the second is robust to any one. We finally compare these two algorithms to delay-optimized differential detectors which do not require any Doppler shift estimation. We also provide complexity estimations to guide the possible complexity-performance trade-offs.**

***Index Terms*—IoT, CPM, non-coherent detection, Doppler shift**

I. Introduction

Improving the connection of Objects to the Internet (IoT) is possible by relaying the communication through Low Earth Orbits (LEO) satellites [1], especially in areas where setting up gateways is costly. There are two options: use an existing wireless communication standard or design an ad-hoc one [2]. In this paper we are interested in the latter one for the uplink and suggest using a Continuous Phase Modulation (CPM). Its constant envelop enables an optimized energy efficiency of the amplifier which is of utmost importance both for satellites and objects.

This communication segment is affected by Doppler shifts due to the high orbiting speed of LEO satellites. So the detection algorithms should be robust to Doppler shifts. We focus in this article on non-coherent CPM detection which can be grouped into two families depending on the criterion they are based on.

The first one pre-processes the received signal to neutralize the phase contribution making possible the application of the maximum-likelihood criterion for coherent detection on the resulting signal. Numerous papers based on differential pre-processed signals can be found in the state-of-the-art. The common feature is the use of the product of the received baseband signal and a conjugate time-delayed version of it, yielding a signal that is referred to as differential signal. Different algorithms are proposed and applied either on time-discrete differential signals (see e.g. [3]) or on time-continuous differential signals (see e.g. [4]–[8]). The main advantage of differential algorithms is their robustness to Doppler shifts, but the signal-to-noise ratio (SNR) loss can be important depending on the algorithm.

The second non-coherent detection class is derived from the generalized maximum-likelihood criterion [9], [10] and only requires the knowledge of the phase distribution. Algorithms proposed either in [11] or in [12] with an uniformly-distributed phase assumption belong to it. In this article, we propose two algorithms both based on this non-coherent criterion and robust to Doppler shifts. The contributions are (i) a novel CPM non-coherent detection based on the direct application of the generalized maximum likelihood principle (ii) the insertion of blind Doppler estimation principle of [13] in the proposed algorithm as well as in the CPM non-coherent detection of [12] (iii) the comparison of the two resulting receivers with the delay-optimized differential detector of [8] in presence of Doppler shifts. The remainder of the article is organized as follows: model and notations are introduced in Section II. In Section III, we derive the non-coherent detection criterion and the two proposed detection algorithms. Simulation results are provided in Section IV and a conclusion is given in Section V.

This work has been financially supported by Thales Alenia Space and Brest Métropole.

II. System Model and Notations

We consider a sequence of N independent and identically distributed (i.i.d.) information symbols $\mathbf{a} = \{a_i\}_{0 \leq i \leq N-1}$ to be transmitted. Given M an even positive integer, a_i takes on values in the M-ary alphabet $\mathcal{M} = \{\pm 1, \pm 3, .. \pm (M-1)\}$ with equal probabilities. The complex envelope of the CPM-modulated signal is given by:

$$s(t, \mathbf{a}) = \sqrt{\frac{2E_s}{T_s}} \mathrm{e}^{j\theta(t,\mathbf{a})}, \tag{1}$$

where E_s is the average symbol energy, T_s is the symbol period and $\theta(t, \mathbf{a})$ is the signal phase which depends on the information symbols. It is defined by:

$$\theta(t, \mathbf{a}) = 2\pi h \sum_{i=0}^{N-1} a_i q(t - iT_s), \tag{2}$$

where h is the modulation index and $q(t)$ is the phase shaping pulse whose expression is $q(t) = \int_{-\infty}^{t} g(u)du$ with $g(t)$ the frequency waveform. In practice, $g(t)$ has a finite duration LT_s and it must satisfy the following conditions:

$$\begin{cases} g(t) = g(LT_s - t), & 0 \leq t < LT_s \\ \int_{-\infty}^{t} g(\tau)\mathrm{d}\tau = q(LT_s) = \frac{1}{2}, & \forall t \geq LT_s \end{cases} \quad (3)$$

We consider a Gaussian transmission channel which introduces a phase rotation of the modulated signal equal to $2\pi f_D t + \phi$ (Doppler shift). The phase ϕ is modeled as a random variable with a uniform distribution in $[0, 2\pi[$ and the frequency shift f_D is constant. The baseband equivalent received signal, denoted $r(t)$, is given by:

$$r(t) = s(t, \mathbf{a})e^{j(2\pi f_D t + \phi)} + \eta(t), \quad (4)$$

where $\eta(t)$ is the realization of a zero-mean wide-sense stationary complex circularly symmetric Gaussian noise, independent of the signal, and with double-sided Power Spectrum Density $2N_0$.

III. Detection strategy

The detection strategies proposed in this article are based on the generalized maximum-likelihood [9] that we shall recall below. Let T_0 be the observation interval of the signal $r(t)$ and let $\mathcal{A}$ designate the set of possible symbol sequences, $\mathcal{F}$ the variation interval of f_D and I_0 the modified first-order Bessel function.

The generalized maximum-likelihood method [9] is used for a blind Doppler shift estimation in conjunction with symbol detection and consists in maximizing the following cost function

$$\begin{aligned} \Gamma(\tilde{\mathbf{a}}, \widetilde{f_D}) &= \log \mathrm{I}_0 \left(\frac{1}{N_0} \left| \int_{T_0} r(t, \mathbf{a}) s^*(t, \tilde{\mathbf{a}}) e^{-j2\pi \widetilde{f_D} t} dt \right| \right) \\ &\quad - \frac{1}{2N_0} \int_{T_0} |s(t, \tilde{\mathbf{a}})|^2 dt \end{aligned} \quad (5)$$

over $\mathcal{A} \times \mathcal{F}$. This is equivalent to:

$$\max_{\tilde{\mathbf{a}} \in \mathcal{A}} \Gamma(\tilde{\mathbf{a}}, \widehat{f}_D(\tilde{\mathbf{a}})) \quad (6)$$

with $\widehat{f}_D(\tilde{\mathbf{a}}) = \arg\max_{\widetilde{f_D} \in \mathcal{F}} \left| \int_{T_0} r(t) s^*(t, \tilde{\mathbf{a}}) e^{-j2\pi \widetilde{f_D} t} dt \right|$.

In the following, we apply criterion (6) according to two alternative algorithms. The first (denoted A), based on a linear decomposition of the CPM, is a combination of the methods described in [12] (denoted NSD algorithm) and [13]. The second (called B) is a sub-optimal algorithm for deriving the criterion directly from (1).

A. Receiver A based on the linear decomposition of CPM

This receiver combines the non-coherent CPM detection algorithm [12] with the Doppler estimation and joint detection algorithm applied to a linear modulation [13]. We consider a linear decomposition of the CPM modulation [14], [15] to get an approximation of the modulated signal: $s(t, \mathbf{a}) \simeq \sum_{k=0}^{K-1} \sum_{i=0}^{N-1} \alpha_{k,i} h_k(t - iT_s)$ where K is the number of principal components, $h_k(t)$ the impulse response of the k-th linear filter and $\alpha_{k,i}$ a symbol defined from $\mathbf{a}$ (see [15] for exact expressions).

The receiver consists of a cascade of a filter bank where filters are adapted to $h_k(t)$, followed by a sampler at period T_e, and a whitening filter.

T_e should be small enough to assume that the samples are a sufficient statistic [16]. However, for a moderate frequency offset ($f_D T_s \ll 1$), $T_e = T_s$ is small enough.

The sampler outputs are given by:

$$x_{k,n} = r(t, \mathbf{a}) \otimes h_k(-t)|_{t=nT_s} \simeq s_{k,n} e^{j(2\pi f_D n T_s + \phi)} + \eta_{k,n}$$

where

$$s_{k,n} = \sum_{m=0}^{K-1} \sum_{i} \alpha_{m,i} p_{m,k}((n-i)T_s), \quad (7)$$

with $p_{m,k}(t) = h_m(t) \otimes h_k(-t)$ and $\eta_{k,n} = \eta(t) \otimes h_k(-t)|_{t=nT_s}$. We introduce the notation $\mathbf{x}_n = (x_{0,n}, x_{1,n}, ..., x_{K-1,n})^T$ and define $\mathbf{s}_n$, $\boldsymbol{\alpha}_n$ and $\boldsymbol{\eta}_n$ likewise. We will also use the discrete impulse response matrices $\mathbf{P}_n = [p_{i,j}(nT)]$ for $i, j = 0, 1, ..., K-1$. With these notations, the observation vector reads:

$$\mathbf{x}_n \simeq e^{j(2\pi f_D n T + \phi)} \sum_{l=-L_w}^{L_w} \mathbf{P}_l^T \boldsymbol{\alpha}_{n-l} + \boldsymbol{\eta}_n, \quad (8)$$

where L_w is a parameter that depends on L.

As the noise samples $\eta_{k,n}$ are correlated, a multidimensional whitening filter (WMF) is implemented [12]. It is specified by the sequence of matrices $\{\mathbf{W}_l\}_{0 \leq l \leq L_w}$. The WMF output observation vector, denoted by $\mathbf{z}_n$, is given by:

$$\begin{aligned} \mathbf{z}_n &= \sum_{l=0}^{L_w} \mathbf{W}_l \mathbf{x}_{n-l} \\ &= e^{j(2\pi f_D n T_s + \phi)} \sum_{l=0}^{L_w} \mathbf{W}_l \mathbf{s}_{n-l} e^{-j2\pi l f_D T_s} + \mathbf{w}_n, \end{aligned} \quad (9)$$

where $\mathbf{w}_n = \sum_{l=0}^{L_w} \mathbf{W}_l \boldsymbol{\eta}_{n-l}$.

Going back to the detection criterion, we apply two approximations. The first one is to consider $\log I_0(x) \simeq x$. The second one depends on the context: we assumes that $f_D T_s$ is small and that $e^{-j2\pi l f_D T_s} \simeq 1$ in the expression (9) of $\mathbf{z}_n$. Given a sequence $\tilde{\mathbf{a}}$ of symbols in $\mathcal{A}$, we define $\tilde{\mathbf{s}}_n$ with (7) and finally $\tilde{\mathbf{y}}_n = \sum_{l=0}^{L_w} \mathbf{W}_l \tilde{\mathbf{s}}_{n-l}$.

The likelihood function calculated in the joint symbol detection and Doppler estimation algorithm is:

$$\begin{aligned} \Gamma_N(\tilde{\mathbf{a}}, \widehat{f}_D(\tilde{\mathbf{a}})) &= \left| \sum_{k=0}^{K-1} \sum_{n=0}^{N-1} z_{k,n} \tilde{y}_{k,n}^* e^{-j2\pi n \widehat{f}_D(\tilde{\mathbf{a}}) T_s} \right| \\ &\quad - \frac{1}{2} \sum_{k=0}^{K-1} \sum_{n=0}^{N-1} |\tilde{y}_{k,n}|^2. \end{aligned} \quad (10)$$

Maximizing (10) involves prohibitive complexity in practice. We adapt the procedure used in [13] to deal with linear

modulations. A Viterbi algorithm is applied associated with a windowing of size N_v for the detection of symbols, a windowing of size $N_D \geq N_v$ for the blind estimation of the Doppler shift and an approximation of $\Gamma_N(\tilde{\mathbf{a}}, \widehat{f}_D(\tilde{\mathbf{a}}))$ by $\Delta_N(\tilde{\mathbf{a}})$ which is calculated in an iterative way as follows:

$$\Delta_n(\tilde{\mathbf{a}}_n) = \Delta_{n-1}(\tilde{\mathbf{a}}_{n-1})) + \lambda_n(\tilde{\mathbf{a}}_\mathbf{n}) \tag{11}$$

with the branch metric being

$$\begin{aligned}\lambda_n(\tilde{\mathbf{a}}_\mathbf{n}) &= \left|\sum_{k=0}^{K-1}\sum_{i=0}^{N_v-1} z_{k,n-i}\tilde{y}^*_{k,n-i}e^{-j2\pi(n-i)\widehat{f}_D(\tilde{\mathbf{a}}^n_{n-N_D}))T_s}\right| \\ &- \left|\sum_{k=0}^{K-1}\sum_{i=1}^{N_v-1} z_{k,n-i}\tilde{y}^*_{k,n-i}e^{-j2\pi(n-i)\widehat{f}_D(\tilde{\mathbf{a}}^n_{n-N_D}))T_s}\right| \\ &- \left|\sum_{k=0}^{K-1}\tilde{y}_{k,n}\right|^2 .\end{aligned}$$

The state at time $n-1$ is defined by the vector $\left(\tilde{\mathbf{y}}^T_{n-1} \ \cdots \ \tilde{\mathbf{y}}^T_{n-N_v+1}\right)^T$, which implies a total of $S = M^{N_v+L_w-1}$ states. As in [13], a *per-survivor processing* (PSP) approach enables to estimate $\widehat{f}_D(\tilde{\mathbf{a}}^n_{n-N_D})$ based on $\tilde{a}_n$ and the partial sequence $\tilde{\mathbf{a}}^{n-1}_{n-N_D} = (\tilde{a}_{n-1} \ \ldots \ \tilde{a}_{n-N_D+1})$ associated to the surviving path at state level at time $n-1$. The data-aided (DA) estimation algorithms proposed for linear phase modulations in [17] are easily applied to the CPM case.

B. Receiver B based on the exact expression of CPM

Considering the constant envelope of the CPM waveform, the likelihood function (6) becomes:

$$\Lambda(\tilde{\mathbf{a}}) = \Gamma(\tilde{\mathbf{a}}, \widehat{f}_D(\tilde{\mathbf{a}})) = \left|\int_{T_0} r(t,\mathbf{a})s^*(t,\tilde{\mathbf{a}})e^{-j2\pi\widehat{f}_D(\tilde{\mathbf{a}})t}dt\right|$$

Let $t_k = kT_s$ and let $v_n(t,\tilde{\mathbf{a}}) = r(t,\mathbf{a})e^{-j2\pi\widehat{f}_D(\tilde{\mathbf{a}}^n_{n-N_D})t}$. To reduce the complexity, we apply the iterative approximation of $\Lambda(\tilde{\mathbf{a}})$ under the same principles of windowing and of definition of the cumulative and branch metrics:

$$\lambda_n(\tilde{\mathbf{a}}) = \Gamma_n(\tilde{\mathbf{a}}) - \left|\int_{(n-N_v)T_s}^{(n-1)T_s} v_n(t,\mathbf{a})s^*(t,\tilde{\mathbf{a}})dt\right| \tag{12}$$

where $\Gamma_n(\tilde{\mathbf{a}}) = \left|\int_{t_{n-N_v}}^{t_n} v_n(t,\tilde{\mathbf{a}})s^*(t,\tilde{\mathbf{a}})dt\right|$.

With the same reasoning, the search for the sequence maximizing the likelihood function (5) is done using a Viterbi algorithm executed on a trellis whose states at time n correspond to all the possible realizations of $s(t,\tilde{\mathbf{a}}^n_{n-N_v+1})$. The estimation $\widehat{f}_D(\tilde{\mathbf{a}}^n_{n-N_D})$ is done as for receiver A using the PSP approach on a window of length N_D.
The development of the first term of the equation (12) leads to:

$$\Gamma_n(\tilde{\mathbf{a}}) = \sqrt{\frac{2E_s}{T_s}}\left|\sum_{m=0}^{N_v-1}\int_{t_{n-m-1}}^{t_{n-m}} v_n(t,\tilde{\mathbf{a}})e^{-j\theta(t,\tilde{\mathbf{a}})}dt\right| . \tag{13}$$

The term depending on $\theta(t,\tilde{\mathbf{a}})$ in the interval $[t_{n-m-1}, t_{n-m}]$ can be simplified:

$$\theta(t,\tilde{\mathbf{a}}) = 2\pi h\sum_{u=0}^{n-m-1}\tilde{a}_u q(t-uT_s) = \Theta(t,\tilde{\mathbf{a}}) + \pi h\sum_{u=0}^{n-m-L-1}\tilde{a}_u \tag{14}$$

with $\Theta(t,\tilde{\mathbf{a}}) = 2\pi h\sum_{u=n-m-L}^{n-m-1}\tilde{a}_u q(t-uT_s)$.
By replacing (14) in (13), and after some straightforward calculations, we come up with:

$$\Gamma_n(\tilde{\mathbf{a}}) = \sqrt{\frac{2E_s}{T_s}}\left|\sum_{m=0}^{N_v-1} e^{-j\pi h\sum_{u=n-N_v-L+2}^{n-m-L-1}\tilde{a}_u} I_m(\tilde{\mathbf{a}})\right|$$

with $I_m(\tilde{\mathbf{a}}) = \int_{t_{n-m-1}}^{t_{n-m}} v_n(t,\tilde{\mathbf{a}})e^{-j\Theta(t,\tilde{\mathbf{a}})}dt$.
We deduce that the computation of $\lambda_n(\tilde{\mathbf{a}})$ depends only on $[\tilde{a}_{n-1}, .., \tilde{a}_{n-N_v-L+2}]$. The Viterbi algorithm therefore applies to a trellis with $S = M^{N_v+L-2}$ states (number of realizations of $[\tilde{a}_{n-1}, .., \tilde{a}_{n-N_v-L+2}]$).

IV. PERFORMANCES

In this Section, an evaluation in terms of simulated error rates and complexity estimation is proposed for the two algorithms A and B. These performances will also be compared to differential detection based decoders [8] which are robust to any constant Doppler shift. Differential detection is built on the generation of a differential signal which is obtained by multiplying the received signal with its delayed version. The considered delay is given by the number K of symbols and is usually $K = 1$. However, performances can be improved by optimizing K as proposed in [8]. In the following, notation K_{opt} will refer to the optimized value of K according to [8].

A. Bit Error Rates Comparison

In this section, bit error rates (BER) are estimated through Monte-Carlo simulations as a function of the ratio E_b/N_0 where E_b denotes the average information bit energy. To this aim, we take into account the overhead used for initialization and estimation in the calculation of E_b/N_0.
We illustrate the error rate performance by first considering the GMSK waveform in Figure 1, with $BT = 0.25$ and $L = 2$ to transmit short frames of $N = 120$ symbols. The symbol duration is fixed to $T_s = 10^{-4}$s. The blind estimation of f_D in detectors A and B is obtained by an algorithm from Rife and Boorstyn [17]. For detector A, we proceed as in [18] by keeping only the first of the principal components resulting from the linearization of the GMSK leading to a one-dimensional whitening filter ($K = 1$) with $L_w = 2$. In the simulations, the choice of $N_v = 5$ and $N_D = 8$ proved to be the best trade-off between complexity and performance for both detectors.

For a small Doppler shift $f_D T_s = 0.05$, detector A and B perform nearly the same with a loss of 1 dB compared to the NSD performance which correspond to the performance without any Doppler shift. When the Doppler shift is increased to $f_D T_s = 0.1$, the performance of detector A is degraded and a gap of 3 dB compared to the NSD is observed at a BER of 10^{-4}. Indeed, when the Doppler shift increases,

the assumption of sufficient statistics does not hold anymore. This is not the case with detector B whose performance is only limited by the capabilities of the Doppler shift estimation algorithm. In fact, with a perfect Doppler shift estimation, the detector B and NSD curves are superimposed.

Differential detectors are insensitive to the Doppler shift and exhibit the same error rate whatever the value of f_D. We observe that $f_D T_s = 10^{-1}$ is the threshold beyond which the BER curve of the differential detection with optimized delay crosses the BER curve of Detector B at a BER of 2.10^{-5}. The error rate comparison between Detector B and differential detections for a 3REC CPM with $h = 0.75$ is illustrated in Figure 2 using the same Doppler shift estimation as for the previous GMSK case (same frequency resolution size). We observe that the gap to NSD is however higher (about 3 dB for a BER of 10^{-3}). We also observe that the performance of differential detection with optimized delay peforms better below a BER of 10^{-2}. It is of course possible to improve the gap between Detector B and NSD by improving the Doppler shift estimation, yielding a higher complexity. In the following, a complexity estimation is proposed to unveil the best performance-complexity trade-offs.

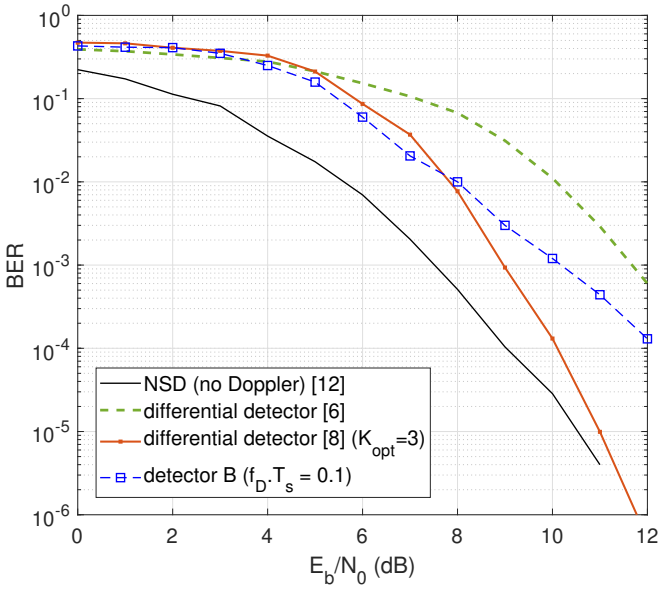

Fig. 2. Comparison of detector B with optimized-delay differential detector [8] for CPM 3REC with $h = 0.75$ - $N_v = 5$, $N_D = 8$, $\rho = 8$ and $N_{\mathrm{FFT}} = 256$

B. Complexity Estimation

In this Section, we propose to estimate the complexity of detectors in terms of the number of trellis states (S), the number of multiplications for metric calculation (Q_M) per trellis section and the number of multiplications for Doppler Shift estimation per trellis section (Q_D). The complexity of the three detectors is summarized in the Table I.

Detector A based on Laurent's decomposition enables sampling at symbol time if the Doppler frequency shift remains moderate. The calculation of branch metrics amounts to $N_v M^{N_v+L_w}$ multiplications per trellis section, while the matched filtering involves $(L_w+1)K^2$ per trellis section.

TABLE I
COMPARISON OF THE DETECTORS IN TERMS OF COMPLEXITY (NUMBER OF STATES S, NUMBER OF MULTIPLICATIONS PER TRELLIS SECTION FOR DETECTION Q_M AND NUMBER OF MULTIPLICATIONS PER TRELLIS SECTION FOR DOPPLER ESTIMATION Q_D)

Label	Detector A	Detector B	Differential detector [8]
S	$M^{N_v+L_w-1}$	M^{N_v+L-2}	$M^{K_{\mathrm{opt}}+L-1}$
Q_M	$(L_w+1)K^2 + N_v SM$	$\rho N_v SM$	ρSM
Q_D	$\rho S(N_D+M-1) + MS\frac{N_{\mathrm{FFT}}}{2}\log_2(N_{\mathrm{FFT}})$		none

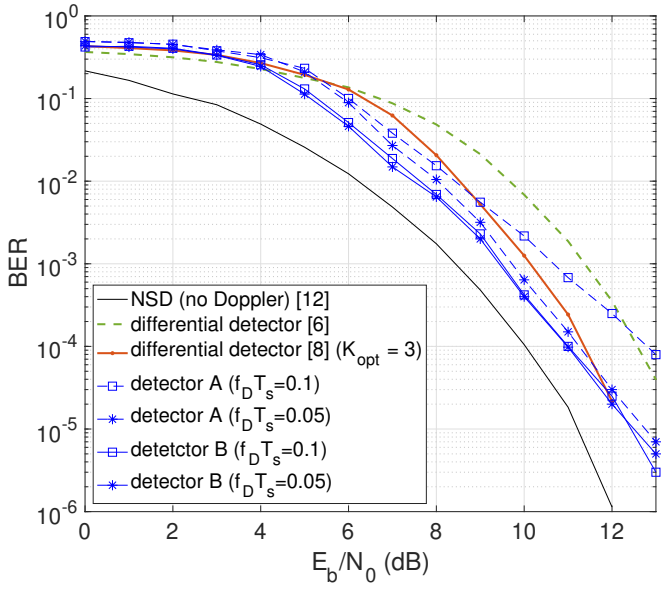

Fig. 1. Comparison of detectors A ($\rho = 1$, $N_{\mathrm{FFT}} = 32$) and B ($\rho = 8$, $N_{\mathrm{FFT}} = 256$) with optimized-delay differential detector [8] for GMSK - $N_v = 5$, $N_D = 8$

In the case of detector B, the multiplications come solely from the branch metric calculations. The numerical calculation of the integral requires a discretization of the signal. Assuming it is done with ρ samples per symbol time, the total number of multiplications per trellis section is given by $\rho N_v M^{N_v+L-1}$.

Both detectors A and B use the Rife and Boorstyn [17] algorithm to blindly estimate the Doppler shifts. Its implementation uses *Fast Fourier Transform* (FFT) on a vector of ρN_D samples ($\rho = 1$ for detector A) obtained by multiplying the received signal with the complex conjugate of the signal reconstructed from the last N_D symbols using the PSP approach (amounting to $S\rho(N_D-1) + MS\rho$ multiplications). Zero padding this vector up to N_{FFT} samples is used to increase the FFT resolution and thus the blind Doppler shift estimation resolution which affects the overall performance (amounting to $MS\frac{N_{\mathrm{FFT}}}{2}\log_2(N_{\mathrm{FFT}})$ multiplications).

The optimized-delay differential detector is also based on a trellis and the calculation of its metrics requires oversampling the signal as well, that is ρ samples per symbol time. The

TABLE II
NUMERICAL VALUES OF S, Q AND E FOR GMSK

Label	Detector A (N_{FFT}=32)	Detector B (N_{FFT}=256)	Differential detector [6] ($K=1$)	Differential detector [8] ($K_{\mathrm{opt}}=3$)
S	64	32	4	16
Q_M	643	2560	64	256
Q_D	10816	67840	NA	NA

number of multiplications is then given by $\rho M^{K_{\mathrm{opt}}+L}$ and no Doppler estimation is needed for the differential detector.

Table II summarizes the numerical values of S, Q_M and Q_D used in our simulations in the case of GMSK with $\rho = 8$. $N_{\mathrm{FFT}} = 32$ for detector A and $N_{\mathrm{FFT}} = 32 \times \rho = 256$ for detector B so that the frequency resolution is the same.

Considering both complexity and error rates, we can state that differential detection with optimized delay from [8] is to be chosen in the high SNR regime or if low complexity is mandatory. If the constraint on complexity is a bit relaxed and lower SNR is considered, then detector A can be chosen if the Doppler shift is small. For larger Doppler shifts and low SNR, improved performance can be obtained close to the non-Doppler case with Detector B while increasing the complexity (both on the metric part and on the Doppler estimation part). The thresholds involved in this comparison do depend on the considered CPM parameters.

V. CONCLUSION

In this article, we proposed two CPM detectors robust to phase uncertainty and Doppler shift. The first one (A) is adapted from a non-coherent CPM detection based on a linear decomposition that we complemented by a blind Doppler shift estimation part. The second one (B) is directly derived from the non-coherent detection criterion applied to the CPM waveform. The simulation results confirm the robustness of these detectors to small Doppler shifts, and to higher Doppler shifts for Detector B for which the only limitation is the performance of the blind Doppler shift estimator. Detector A and B are also compared to differential detectors. When an optimized delay is used, differential detection performs better in the high SNR / low error rate regime, while keeping a low complexity: differential detection does not include any Doppler shift estimation. As far as a lower SNR regime is concerned, provided that complexity is not an issue, Detector A for low Doppler shifts and Detector B otherwise offer better performances.

REFERENCES

[1] Z. Qu, G. Zhang, H. Cao, and J. Xie, "LEO satellite constellation for Internet of Things," *IEEE Access*, vol. 5, pp. 18 391–18 401, 2017.

[2] J. A. Fraire, S. Céspedes, and N. Accettura, "Direct-to-satellite IoT - a survey of the state of the art and future research perspectives," in *Ad-Hoc, Mobile, and Wireless Networks*. Springer Int. Publishing, 2019, pp. 241–258.

[3] G. Kawas Kaleh, "Differential detection of partial response continuous phase modulation with index 0.5," in *IEEE 39th Vehicular Technology Conference*, 1989, pp. 115–121 vol.1.

[4] D. Makrakis and P. Mathiopoulos, "Differential detection of correlative encoded continuous phase modulation schemes using decision feedback," in *IEEE Int. Conf. on Communications*, 1990, pp. 619–625 vol.2.

[5] M. Simon and C. Wang, "Differential versus limiter - discriminator detection of narrow-band fm," *IEEE Transactions on Communications*, vol. 31, no. 11, pp. 1227–1234, 1983.

[6] N. Svensson and C.-E. Sundberg, "Performance evaluation of differential and discriminator detection of continuous phase modulation," *IEEE Transactions on Vehicular Technology*, vol. 35, no. 3, pp. 106–117, 1986.

[7] D. Makrakis and K. Feher, "Multiple differential detection of continuous phase modulation signals," *IEEE Transactions on Vehicular Technology*, vol. 42, no. 2, pp. 186–196, 1993.

[8] A. Jerbi, K. Amis, F. Guilloud, and T. Benaddi, "Delay Optimization of Conventional Non-Coherent Differential CPM Detection," April 2022, available at https://arxiv.org/abs/2204.05826.

[9] H. L. V. Trees, *Detection, estimation and modulation theory*. New York: John Wiley & Sons, vol. I, 1968.

[10] C. Piat-Durozoi, C. Poulliat, N. Thomas, M. Boucheret, G. Lesthievent, and E. Bouisson, "Minimal State Non-Coherent Symbol MAP Detection of Continuous-Phase Modulations," *IEEE Communication Letters*, vol. 22, no. 10, pp. 2008–2011, 2018.

[11] M. Simon and D. Divsalar, "Maximum-likelihood block detection of noncoherent continuous phase modulation," *IEEE Transactions on Communications*, vol. 41, no. 1, pp. 90–98, 1993.

[12] G. Colavolpe and R. Raheli, "Noncoherent sequence detection of continuous phase modulations," *IEEE Trans. on Commun.*, vol. 47, no. 9, pp. 1303–1307, 1999.

[13] G. Colavolpe, R. Raheli, and G. Picchi, "Detection of linear modulations in the presence of strong phase and frequency instabilities," in *IEEE Int. Conf. on Communications.*, vol. 2, 2000, pp. 633–637.

[14] P. Laurent, "Exact and approximate construction of digital phase modulations by superposition of amplitude modulated pulses (AMP)," *IEEE Trans. on Commun.*, vol. 34, no. 2, pp. 150–160, 1986.

[15] U. Mengali and M. Morelli, "Decomposition of M-ary CPM signals into PAM waveforms," *IEEE Trans. on Inf. Theory*, vol. 41, no. 5, pp. 1265–1275, 1995.

[16] H. Meyr, M. Oerder, and A. Polydoros, "On sampling rate, analog prefiltering, and sufficient statistics for digital receivers," *IEEE Trans. on Commun.*, vol. 42, no. 12, pp. 3208–3214, 1994.

[17] M. Morelli and U. Mengali, "Feedforward frequency estimation for PSK: a tutorial review," *Eur. Trans. Telecommun.*, vol. 9, pp. 103–116, 1998.

[18] G. Colavolpe and R. Raheli, "Noncoherent sequence detection," *IEEE Trans. on Commun.*, vol. 47, no. 9, pp. 1376–1385, 1999.